Latent Social Distancing
Identification, Causes and Consequences

M. Aykut Attar* Ayça Tekin-Koru†

June 2, 2020

Abstract. This paper derives a **M**odel-**I**nferred **DIS**tancing (MIDIS) measure using an extended version of the Susceptible-Exposed-Infected-Recovered-Deceased (SEIRD) framework. The paper argues that, when a disease has an incubation period, explicitly accounting for the exposed compartment is necessary in this class of epidemiological models. An important advantage of the proposed identification strategy lies in its ease to put into practice by other researchers because it employs a relatively simple model and readily available data. When MIDIS is taken to data, results exhibit cross-country and over-time heterogeneity in social distancing during the COVID-19 pandemic. Furthermore, MIDIS is highly correlated with the mobility data, and it embeds both governmental and behavioral responses to the COVID-19 pandemic. Finally, as an application, the paper uses MIDIS to explain output losses experienced during the pandemic, and there exists a robust positive correlation between the two—with sizable economic effects.

JEL Codes. C02 • D91 • I18

Keywords. SEIRD • social distancing • COVID-19 • output loss

Acknowledgments. We wish to thank Ben McWilliams and Georg Zachmann for sharing their daily electricity data with us. Any remaining errors are our own.

* Dept. of Economics, FEAS, Hacettepe University, Beytepe Campus, 06800 Cankaya/Ankara, Turkey, Tel.: +90-312-2978650 (Ext: 135), maattar@hacettepe.edu.tr

† Dept. of Economics, TED University, Ziya Gökalp Caddesi, No.47, 06420 Cankaya/Ankara, Turkey, Tel.: +90-312-5850034, ayca.tekinkoru@tedu.edu.tr

1. Introduction

The COVID-19 pandemic has already enveloped the planet in its entirety and triggered a wide range of containment or distancing measures in almost all parts of the world. These measures have resulted in a serious economic downturn with the potential to dwarf the Great Depression. As of June 1, 2020, the disease claimed nearly 375,000 lives, and the case numbers reached more than 6 million worldwide with no vaccine or antiviral therapy in close sight.

The only available instrument to slow down the rate of infection was and continues to be social distancing, which can be loosely defined as a set of non-pharmaceutical interventions (NPIs) to reduce person-to-person contact. These interventions can be taken by governments or individuals and serve the objective of "flattening the epidemiological curve," a plot of the number of new cases per day. Theoretical reasoning suggests that the social return to distancing exceeds its private return, thereby necessitating policy interventions (e.g., Bethune and Korinek, 2020; Farboodi et al., 2020).

Social distancing to "flatten the curve" unequivocally creates a plethora of economic shocks. But which countries have experienced the highest rates of increase in social distancing, and what is the extent of social distancing? These questions are imperative for understanding what triggers economic tremors felt all over the world, yet we know remarkably little about social distancing that has the power of creating major economic downturns. Why? Because, it belongs to a set of *intrinsically latent variables* which are typically well understood but rarely rigorously defined (Kmenta, 1991). Unlike a proxy variable, an *intrinsically latent variable* is unobserved and never characterized by just one measurable factor. Hence, it can only be inferred from other observable variables using formal (mathematical) theory that provides identification restrictions.

This paper sheds light on these issues by developing a way of identifying unobserved social distancing and aims to contribute to the vivid debate on "flattening the curve," cross-country heterogeneity in the effectiveness of governmental and behavioral responses, and economic costs of the pandemic.

In the first part of the paper, we derive a **M**odel-**I**nferred **DIS**tancing (MIDIS) measure using an extended version of the workhorse **S**usceptible-**E**xposed-**I**nfected-**R**ecovered-**D**eceased (SEIRD) framework.[1] In the typical SEIRD model, there is a nonlinear dynamical system that explains the spread and eventual containment of an infection over time. In this paper, we extend the simple SEIRD model with a time-varying and country-dependent social distancing term. The core idea of our paper is to identify this distancing term, MIDIS, for each country and each day by exploiting the fact that the pure probability of transmission and the average incubation period are constant and common across countries. The resulting solution expresses MIDIS as a function of observable epidemiological data and thus provides a model-inferred measure of a latent variable that can be tracked over time. An important

1 The model was originally proposed as a SIR model by Kermack and McKendrick (1927) and, later, various extensions with stochastic specifications and more compartments were produced. We briefly review that literature below.

advantage of our identification strategy lies in its ease to put into practice by other researchers because it employs a relatively simple epidemiological model and readily available data.

To the best of our knowledge, Fernández-Villaverde and Jones's (2020) paper is the closest one to ours with respect to identification. These authors also use a compartmental model (the SIRD version) and daily epidemiological data, and their identification strategy of recovering time-varying transmission rate using observables is similar to our identification of distancing. However, there are four substantial differences. First and the foremost, our model has the exposed compartment between the Susceptible and Infected compartments whereas Fernández-Villaverde and Jones (2020) implicitly assume that the exposed individuals are in the Susceptible compartment. Second, while both papers use the daily epidemiological data on the numbers of deceased and recovered individuals, we use observed data of country-dependent and time-varying recovery and fatality rates in identification. In contrast, Fernández-Villaverde and Jones (2020) assign fixed and country-independent values to several model parameters (but of course do so rigorously). Third, our approach exploits the fact that the pure probability of transmission is fixed and common across countries and thus identifies the unobserved distancing term directly for each country and day. Fernández-Villaverde and Jones (2020), however, identify the effective transmission rate directly, and they do not put an effort to differentiate the distancing term from pure probability of transmission. Finally, our paper focuses on the identification, causes, and economic consequences of distancing, but Fernández-Villaverde and Jones (2020) use their model and the recovered sequences of time-varying transmission rates to understand the evolution of death rates and the progression of the pandemic in the near future. We believe that explicitly accounting for the exposed compartment is necessary since COVID-19 has a strictly positive average incubation period. Besides, our approach of utilizing observed changes in recovery and fatality rates allows us in understanding the evolution of distancing during the pandemic.

One advantage of our identification strategy is that MIDIS captures a wide range of social distancing components. These include not only policy interventions (school/work closures, bans on traveling and mass gatherings or stay-home orders) but also behavioral responses such as fear, trust, or reciprocity which cannot be measured in a straightforward way. As underlined by Toxvaerd (2020), modeling how people behave during a pandemic (under the presence of distancing interventions) by exogenously given diffusion parameters is not sufficient for the analysis of disease control. There exists an endogenous response of human behavior to a highly contagious disease—embodied in every day social interactions—that needs to be accounted for in epidemiological models.

While it would be the first-best to collect direct data on different components of social distancing, this is hardly likely in practice due to severe data limitations. The data on policy measures taken to curb the spread of the disease may not always be readily available for a number of countries on a daily basis, let alone the daily data for behavioral responses. MIDIS derived in this paper eschews this problem by providing researchers a measure that is easy to construct. It can be useful not only for studying economic costs but also for other applications that require a time-varying measure of social distancing.

Naturally, our analysis encompasses some of the caveats of SEIRD modeling as well as

measurement errors in the observed data. For the latter problem, it is known that countries are not equally successful in testing and tracking, and data manipulation by official bodies in some countries could cause quantitative results to be misleading to some extent. For the former issue, one of the most serious problems of SEIRD models is the weak identification of model parameters (Avery et al., 2020). As Fernández-Villaverde and Jones (2020) have underlined as well, different constellations of model parameters that have similar fits in the short run—days to weeks—may imply significantly diverse outcomes in the long run—months to years. Our imperfect remedy for this problem is to check the sensitivity of our results, and we show that the evolution of MIDIS is considerably robust under alternative parameter values. Another issue is parameter stability under the presence of policy changes as underlined by Chang and Velasco (2020) with reference to the Lucas critique. Since we do not pursue counterfactual policy analyses, parameter stability is not a central concern for us. The last but not least, the simple models with homogeneous individuals inhabiting a single society may be misleading because of (i) population heterogeneity in age structure, exposure risk, and health status, (ii) the regional differences within a country, and (iii) spatial linkages among the localities. However, currently available data do not allow us to pursue such intriguing dimensions for the moment.

In the second part of the paper, we take MIDIS to the data compiled by Johns Hopkins University (JHU, 2020) and compute it for 44 countries with a total number of confirmed COVID-19 cases that exceeds 10,000 as of May 11, 2020. For the immediate 30-days in the aftermath of the 500th case, our results show that countries exhibit considerable variation with respect to initial social distancing levels. With the exceptions of the US and Spain, countries start with an initial social distancing level that is larger than the Chinese benchmark. Furthermore, in a large number of countries, there is a minor decline of MIDIS within the first week that is followed by a slow yet persistent increase later on. South Korea is the country that sustains the highest average level of distancing, and the US is the least effective country. That there is considerable cross-country variation in social distancing levels and the South Korean success relative to the European countries are consistent with the SIR-based empirical evidence presented by Chudik et al. (2020).

We, then, compare MIDIS values to the mobility data supplied by Apple and Google that have now been used in the burgeoning COVID-19 literature -sometimes as a proxy for social distancing.[2] Our results indicate a highly significant negative correlation between MIDIS values and different components of mobility. The advantage of MIDIS over the mobility data is its wide coverage at country-day detail as long as the epidemiological basic data are available.

In the third part of the paper, we try to identify the cross-country heterogeneity in MIDIS that might be a result of differences in governmental response, behavioral response and a plethora of country-specific factors. We argue that behavioral response to a pandemic is at least as important—if not more—as governmental response in explaining the variation in MIDIS across countries and time. As expected, our results show that our social distancing

2 See Alfaro et al. (2020), Coven and Gupta (2020), Durante et al. (2020), and Doganoglu and Ozdenoren (2020) and the references therein.

measure varies positively with containment measures taken by governments and people's reaction to the pandemic in a robust manner. Indeed, the impact of behavioral response measured by the numbers of deceased on the previous day is stronger than the impact of containment measures. Almost all country-specific variables we use are unsuccessful in explaining the variation in MIDIS. This last result may indicate that the virus—hence social distancing—does not differentiate between developed or otherwise and can manifest itself in unexpected ways compared to our conventional wisdom.

In the final part of the paper, we use our model-inferred social distancing measure to study the economic costs of social distancing during a pandemic. While doing so, we stay oblivious to supply or demand side dynamics of these economic costs and focus on their outcome in terms of output loss only. Our daily measure of output loss is derived from the peak-hour electricity consumption data, generously provided by McWilliams and Zachmann (2020). Our results indicate a significant negative output response to social distancing during the COVID-19 pandemic. In other words, in countries with higher levels of MIDIS, there is a higher level of output loss in the 30-days following the 500th case. Indeed, a 10 percent increase in social distancing causes up to a 3.8 percent increase in output loss.

The paper is structured as follows: Section 2 reviews the related literature. Section 3 introduces the model and our identification strategy. Section 4 summarizes the main patterns of distancing using the identified MIDIS values and validates MIDIS through mobility data. Section 5 investigates the cross-country differences in MIDIS using various explanatory variables. Section 6 then investigates whether and to what extent distancing during the pandemic is related with output losses. Section 7 concludes the paper with some final remarks. We present the results of sensitivity analyses in Appendix A, and variable definitions, data sources, and statistical summaries in Appendix B. Computer codes and MIDIS data can be accessed at the MIDIS website.

2. Related Literature

There is now a large and growing literature studying various economic aspects of the COVID-19 pandemic. As of May 31, 2020, there exist over 70 COVID-19-related research papers documented by the NBER, all written in the last few months.[3] There also exist other outlets where researchers share their recent works on the COVID-19 pandemic. *Covid Economics: Vetted and Real-Time Papers*, published by the Centre for Economic Policy Research since March 2020, has now 24 completed issues containing dozens of papers on the COVID-19 pandemic.

Our purpose in this section is to present a discussion of the related literature by focusing on the papers that are most directly related to ours. Compartmental models such as SIR, SEIR, or SEIRD are useful tools in the mathematical study of infectious diseases. Originally developed by Kermack and McKendrick (1927) in the form of SIR, the (stochastic versions of) models with more compartments (e.g., with the Quarantined or the Hospitalized ones) have been proposed to make the analysis more realistic (e.g., Chowell et al., 2003; Zhou

3 These papers can be accessed at `https://www.nber.org/wp_covid19.html`

et al., 2004; Lekone and Finkenstädt, 2006; Feng, 2007). Most recently, researchers estimated such realistic versions with the Chinese COVID-19 data (Tang et al., 2020; He et al., 2020). In this paper, we focus on the simplest version of a compartmental model that fits our purposes. Hence, we build on a deterministic version that explicitly accounts for the exposed compartment and extend it with time-varying and country-dependent (unobservable) distancing.

Recent work by economists is related to our paper in two respects. First, several papers embed a compartmental epidemiological model (within a dynamic equilibrium framework) to tackle a diversity of research questions. Second, another set of papers empirically investigate the causes and consequences of social distancing, identified or measured/proxied in one way or another.

In the first strand where researchers use a version of a compartmental model, they generally focus on how governmental and behavioral responses affect the progression of the pandemic through distancing. Other than Fernández-Villaverde and Jones (2020) that we have discussed above, there is a large number of papers in this category, and we choose to discuss only some of them for space considerations.

Building on the SIR model, Toxvaerd (2020) designs an optimal control problem at the individual level to solve for daily equilibrium dynamics of social distancing. The model implies that there exists an episode during which the number of infections does not increase as a result of optimal behavioral responses. In a similar fashion, Cochrane (2020) shows simulations of a SIR model where distancing behavior depends on the infection rate or the increase in the death toll as people decrease their exposure under the presence of increasing infection rates or deaths. Acemoglu et al. (2020) extend the SIR model with three age groups that face different levels of mortality risks and show that targeted policies are more effective than uniform policies in terms of both economic costs and health outcomes. Authors also emphasize the sizable positive effects of group distancing that isolates the most vulnerable from the rest of the society. Alvarez et al. (2020) also use the SIR model and study the optimal control problem of lockdown policies. The optimal policy they find depends on the fractions of susceptible and infected individuals, and it prescribes a severe initial lockdown and a gradual withdrawal of it in months. Berger et al. (2020) extend a SEIR model with incomplete information, testing, and quarantine policies. They find that targeted quarantine policies with higher testing rates are effective in mitigating the adverse economic and epidemiological effects. Eichenbaum et al. (2020) embeds the SIR model within a typical dynamic macroeconomic model to study the effects of various policy responses. In their SIR-macro model, individuals' distancing decisions that decrease their consumption and labor supply have positive health impacts but increase the size of economic downturn. Another modeling exercise pursued by Kaplan et al. (2020) incorporates the SIR model within a New Keynesian model with heterogeneous agents (HANK). Authors underline the differential impact of the pandemic across different types of consumer goods and occupations, and they also show that the ownership structure of liquid versus illiquid assets matters because the group of individuals that are most exposed to economic risks have lowest liquidity.

Our paper benefits from this literature in motivating the roles of governmental and behavioral responses to the pandemic; our empirical results—confirming that governmental

and behavioral responses drive effective distancing—have a strong theoretical basis. However, our approach differs from all these papers in two respects: First, a vast majority of the papers ignore the role of the exposed compartment but realistic epidemiological studies of the COVID-19 pandemic necessitates a S"E"IRD framework (He et al., 2020; Tang et al., 2020). Second, instead of investigating whether a particular policy or behavior is optimal, we remain agnostic about such a counterfactual question and assume that the observed epidemiological data reflect the decentralized equilibrium of distancing. The presumption that the observed data must be consistent with a SEIRD model then allows for the identification of distancing during the pandemic.

The second strand of literature we discuss here focuses more on the empirics of distancing and disease progression, and more specifically on whether governmental and/or behavioral responses are statistically associated with increased distancing and decreased mobility.

Chen and Qiu (2020) and Castex et al. (2020) investigate the role of governmental responses on the infection rates by recovering the daily infection rates from a SIR model. The former paper designs different scenarios using NPIs for nine countries and shows that school closures, mask wearing, and centralized quarantine measures are effective in reducing the transmission rates. Authors also show that these three measures have quantitatively similar effects when compared with a strict lockdown. The latter paper implements the analysis for a large number of countries and finds that GDP per capita, population density, and surface area decrease policy effectiveness.

Doganoglu and Ozdenoren (2020) investigate the role of trust and social norms on behavioral responses to the pandemic. They first isolate the effects of (i) policy measures using the Stringency Index of Hale et al. (2020), (ii) the number of infections, and (iii) the temperature on people's mobility using the Google (2020) data. They then estimate the role of trust on the country fixed effects that cannot be explained by policies, infections, and temperature. Their results indicate that, while policies and infections decrease mobility levels, trust has a positive impact on mobility. Alfaro et al. (2020) also focus on behavioral responses motivated by fear, altruism, and reciprocity, and they investigate the effects of both policy measures and these traits. Their empirical results that utilize Apple (2020) mobility data show that the effects of policy measures is less pronounced if people are more patient and more altruistic and if they exhibit a lesser degree of negative reciprocity.

The empirical literature also shows that partisanship may be an important dimension in guiding people's distancing behavior. Painter and Qiu (2020) use geolocation data for the US counties to show that people in Democratic counties are more responsive to policy interventions, and Engle et al. (2020) estimate that an official stay-at-home restriction decreases mobility by more than 7 percent in the US. In a separate study (on the US counties), Brzezinski et al. (2020) confirm that the effect is indeed close to 8 percent. In another interesting paper related with partisanship effects, Argentieri Mariani et al. (2020) demonstrate—using an event-study approach and regional variation of vote shares in Brazil—that the president's public disrespect for the recommendations of health authorities has increased the infection rates.

Empirical studies demonstrate that policies are effective in reducing the infection rates and the number of deaths through distancing (Deb et al., 2020; Askitas et al., 2020). How-

ever, estimates also show that people respond to the pandemic by decreasing their mobility to some extent even in the absence of policy interventions (Brzezinski et al., 2020). This result (for the US) has also been supported by the mobility data of Google (2020) in a paper by Maloney and Taskin (2020). These authors also estimate that the effect of voluntary distancing is larger than that of policy interventions for a large number of countries.

Our empirical results are consistent with the main lessons of this literature, namely that both governmental and behavioral responses are significantly associated with distancing and mobility. We should also note that our approach is closer to those of Chen and Qiu (2020), Castex et al. (2020), and Alfaro et al. (2020). Differently from the latter paper, we use a distancing measure originating from an epidemiological model, and, contrary to the first two of these papers, we explicitly account for the exposed individuals in identifying our distancing measure, MIDIS.

3. A SEIRD Model with Distancing

We consider J countries indexed by $j \in \{1, 2, ..., J\}$. The model time, denoted by t, is discrete, and the length of a period is a day. For all countries, the model horizon is the first 30 days after the 500th COVID-19 case is confirmed. Hence, time periods are not synchronized across countries with respect to the calendar time.

The need to restrict our analysis to the period after the 500th case for each country originates from the fact that the official COVID-19 statistics for China starts with 548 cases on January 22, 2020. Furthermore, we choose to restrict the analysis to the first 30 days after 500th case to disregard the effects of partial removal of NPIs.

3.1. Compartments and the Laws of Motion

Following Degue and Le Ny (2018), we study a deterministic version of the SEIRD model where the size of each compartment is expressed as a fraction of population in each country. In this model, susceptible (S) individuals transit to the exposed (E) compartment after being infected, but they stay in the exposed compartment until they become infectious. Individuals in the infected (I) compartment transmit the virus to susceptible individuals, and they either recover (R) or die (D).

Importantly, we extend the basic model with a time-varying transmission rate that is determined by distancing behavior of susceptible and infected populations. Formally, we have

$$S^j_{t+1} = S^j_t - \beta \left[\left(\frac{1 - d^j_t}{\mu} \right) S^j_t \right] \left[\left(\frac{1 - d^j_t}{\mu} \right) I^j_t \right] \tag{1}$$

$$E^j_{t+1} = E^j_t + \beta \left[\left(\frac{1 - d^j_t}{\mu} \right) S^j_t \right] \left[\left(\frac{1 - d^j_t}{\mu} \right) I^j_t \right] - \alpha E^j_t \tag{2}$$

$$I^j_{t+1} = I^j_t + \alpha E^j_t - \gamma^j_{R,t} I_t - \gamma^j_{D,t} I^j_t \tag{3}$$

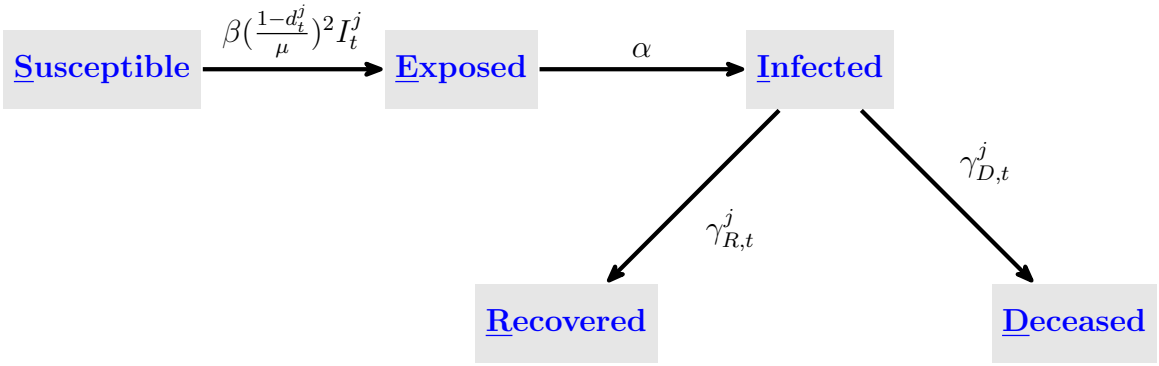

Figure 1: Compartments and Transition Rates in the SEIRD Model

$$R_{t+1}^j = R_t^j + \gamma_{R,t}^j I_t^j \tag{4}$$

$$D_{t+1}^j = D_t^j + \gamma_{D,t}^j I_t^j \tag{5}$$

where S_t^j, E_t^j, I_t^j, R_t^j, and D_t^j denote the fractions of susceptible, exposed (but not infectious), infected (and infectious), recovered, and deceased individuals in country j on day t. By the Law of Large Numbers, each denotes the probability that any given individual is in the associated compartment. Hence, we have

$$S_t^j + E_t^j + I_t^j + R_t^j + D_t^j = 1 \tag{6}$$

for all j and t.

The fixed parameter $\beta \in (0, 1)$ denotes the pure probability of transmission; it is the probability that an infected individual transmits the virus to a susceptible individual if the two get into contact. However, the probability of contact depends on *effective* (or *de facto*) distancing, or MIDIS, denoted by $d_t^j \in [0, 1]$. If both susceptible and infected individuals utilize social distancing instructions, then the probability that a susceptible individual and an infected individual get into contact is equal to

$$\left(\frac{1 - d_t^j}{\mu}\right)^2 S_t^j I_t^j \tag{7}$$

If a country can completely isolate susceptible and infected individuals with $d_t^j = 1$, then no individuals migrate from the susceptible to the exposed compartment. This is the quadratic, one-parameter (μ), one-variable (d_t) formulation that is now familiar in the related literature (Acemoglu et al., 2020; Alvarez et al., 2020). However, the present formulation is slightly different from those of Acemoglu et al. (2020) and Alvarez et al. (2020) since our model features the exposed compartment as well. Here, $\mu > 0$ allows us to identify d_t^j for all countries and all days within the unit interval.[4]

4 In both Acemoglu et al. (2020) and Alvarez et al. (2020), the effect of distancing is introduced via $(1 - \theta L_t)^2$ where $L_t \in [0, 1]$ is the lockdown variable, and $\theta \in [0, 1]$ governs the effectiveness of the lockdown.

Another fixed parameter that is also common across countries is $\alpha \in (0,1)$ that denotes the inverse of the average incubation period of the virus in days. This parameter determines the fraction of exposed individuals that migrate to the infected compartment on any day.

Finally, time-varying fractions of individuals in the infected compartment move to the recovered and deceased compartments on any day. These fractions are denoted by $\gamma^j_{R,t} \in (0,1)$ and $\gamma^j_{D,t} \in (0,1)$, respectively. Figure 1 pictures the compartments and transitions rates in the SEIRD model.

3.2. Identification

Our purpose is to use the above model and observed epidemiological data to achieve a numerical identification of d^j_t for all (j,t). The strategy builds on the notion that, while the pure probability of transmission (β) and the inverse of the average incubation period (α) are fixed and common across countries, there is daily variation in (I^j_t, R^j_t, D^j_t). Hence, the observed data and the model must be consistent with each other for some realization of d^j_t. In other words, we use the model and data to recover d^j_t for any (j,t).

Since whether an infected individual recovers or dies does not matter for d^j_t, we define the compartment X^j_t as the sum of R^j_t and D^j_t as in

$$X^j_t = R^j_t + D^j_t, \tag{8}$$

and we also define $\gamma^j_{X,t} = \gamma^j_{R,t} + \gamma^j_{D,t}$. The SEIX model is then characterized by

$$S^j_{t+1} = S^j_t - (\beta/\mu^2)\left(1 - d^j_t\right)^2 S^j_t I^j_t \tag{9}$$

$$E^j_{t+1} = E^j_t + (\beta/\mu^2)\left(1 - d^j_t\right)^2 S^j_t I^j_t - \alpha E^j_t \tag{10}$$

$$I^j_{t+1} = I^j_t + \alpha E^j_t - \gamma^j_{X,t} I^j_t \tag{11}$$

$$X^j_{t+1} = X^j_t + \gamma^j_{X,t} I^j_t \tag{12}$$

The unobserved state variable that is central to our identification strategy is the ratio of exposed to infected individuals, defined as in $e^j_t = E^j_t / I^j_t$. Notice that (10) and (11) allow us to write the law of motion of e^j_t as in

$$\frac{e^j_{t+1}}{e^j_t} = \frac{(\beta/\mu^2)\left(1 - d^j_t\right)^2 S^j_t (e^j_t)^{-1} + (1-\alpha)}{\alpha e^j_t + (1 - \gamma^j_{X,t})}. \tag{13}$$

The MIDIS term d^j_t for country j on day t can then be written as a function of $(e^j_{t+1}, e^j_t, S^j_t, \gamma^j_{X,t}, \alpha, \beta, \mu)$:

$$d^j_t = 1 - \left[\frac{e^j_{t+1}\alpha e^j_t + e^j_{t+1}(1 - \gamma^j_{X,t}) - (1-\alpha)e^j_t}{(\beta/\mu^2) S^j_t}\right]^{1/2}. \tag{14}$$

Table 1: Confirmed Cases of COVID-19 as of May 11, 2020

Country	Cases	Country	Cases	Country	Cases
USA	1,347,881	Netherlands	42,788	Poland	16,326
Spain	227,436	Saudi Arabia	41,014	Austria	15,882
United Kingdom	223,060	Mexico	36,327	Japan	15,847
Russia	221,344	Pakistan	32,081	Bangladesh	15,691
Italy	219,814	Switzerland	30,344	Ukraine	15,648
France	175,479	Chile	30,063	Romania	15,588
Germany	172,576	Ecuador	29,509	Indonesia	14,265
Brazil	169,594	Portugal	27,679	Colombia	11,613
Turkey	139,771	Sweden	26,670	Philippines	11,086
Iran	109,286	Belarus	23,906	South Korea	10,936
China	84,011	Singapore	23,822	South Africa	10,652
Canada	71,247	Qatar	23,623	Dominican Rep.	10,634
India	70,768	Ireland	23,135	Denmark	10,513
Peru	68,822	UAE	18,878	Serbia	10,176
Belgium	53,449	Israel	16,506		

Source: JHU (2020)

Under the assumption that fixed parameters are known, calculating d_t^j requires the values of $(e_{t+1}^j, e_t^j, S_t^j, \gamma_{X,t}^j)$ for all (j,t).

The model allows us to uniquely identify all of these inputs: (12) identifies $\gamma_{X,t}^j$ for all (j,t) as a function of observed variables $(X_{t+1}^j, X_t^j, I_t^j)$. Then, (11) identifies e_t^j for all (j,t) as a function of observed variables (I_{t+1}^j, I_t^j) and $\gamma_{X,t}^j$. Finally, (6) and (8) identify S_t^j as a function of observed variables (I_t^j, X_t^j) and e_t^j.

4. MIDIS in Selected Countries

We apply our identification strategy to a set of countries that are most seriously affected by the COVID-19 pandemic. At the first step, we select the countries with a total number of confirmed COVID-19 cases that exceeds 10,000 as of May 11, 2020. The source of our daily epidemiological data is the John Hopkins University's COVID-19 data repository (JHU, 2020). The sample includes $J = 44$ countries listed in Table 1.

Next, we apply the Gaussian filter to smooth the original epidemiological data we obtain from JHU (2020). Smoothing is a commonly followed approach in the related literature and necessary for two related reasons: First, since the model we use is deterministic, it is not suitable to capture the noise in the actual data sequences. Second, without smoothing, the identified sequences of e_t^j and $\gamma_{X,t}^j$ for some j and t are not consistent with a real-valued d_t^j term.

Finally, we assign values to the fixed parameters of the model, i.e., (α, β, μ). For α, we borrow the benchmark value from He et al. (2020) and Tang et al. (2020). Both of these papers estimate stochastic versions of a multi-compartment epidemiological model with Bayesian methods using the COVID-19 data of China. In both papers, $\alpha = 1/7$ is

taken as a benchmark value that corresponds to an average incubation period of 7 days. The estimation results of He et al. (2020) additionally show that the pure probability β of transmission is equal to $\beta = 0.111$ with a standard deviation of 0.0015; we adopt this value for our benchmark results. Finally, for the scaling parameter μ, we adopt a value that normalizes the initial value of effective distancing in China to $d_0^{\text{CHN}} = 0.5$. The associated value of μ satisfies $\mu = 0.2376$.

MIDIS values identified using this strategy are not much sensitive to the imposed parameter values; the qualitative properties of MIDIS sequences are not altered for plausible changes in parameters. We present a detailed analysis implemented with alternative parameter values in Appendix A.

In the remainder of this section, we present and discuss two figures. The first one pictures the absolute values of MIDIS in each of the 44 countries in our sample whereas the second one pictures the evolution of *relative* MIDIS defined as in

$$\hat{d}_t^j = \frac{d_t^j}{d_t^{\text{CHN}}} \tag{15}$$

for all (j, t). Here, we take the Chinese case as a benchmark for two related reasons: First, the COVID-19 pandemic has started in China, and there is no better way to compare MIDIS across countries. Second, and more importantly, the pandemic has nearly completed its progression in China in the first half of May 2020. For instance, the smoothed sequence of confirmed cases for China indicates that, for the week ending on May 11, 2020, the average daily growth rate of confirmed cases is equal to 0.0001%.

Figure 2 shows that countries in our sample exhibit considerable variation with respect to initial values and later evolution of MIDIS during the COVID-19 pandemic.

The first thing to note is that most countries with the exceptions of the US and Spain start with an initial value that is larger than the Chinese benchmark of $d_0^{\text{CHN}} = 0.5$. The initial value of the US is nearly 10 percentage points lower than the Chinese level.

The countries that achieve the highest MIDIS values at $t = 0$ of their respective samples include South Africa (0.83), Japan (0.82), Denmark (0.81), and Singapore (0.80). Initial MIDIS values lie between 0.70 and 0.79 for 14 countries, and between 0.60 and 0.69 for 18 countries. Interestingly, for some of the European countries most seriously affected from the COVID-19 pandemic, initial MIDIS values are less than 0.60. These countries are Italy (0.598), France (0.595), United Kingdom (0.584), Turkey (0.560), and Germany (0.504).

Countries differ with respect to the evolution of MIDIS during the first 30 days after the 500th case is confirmed. In some countries, MIDIS remains largely stable; these include Brazil, Colombia, Dominican Republic, Ecuador, Ireland, Mexico, Pakistan, Qatar, and Saudi Arabia.

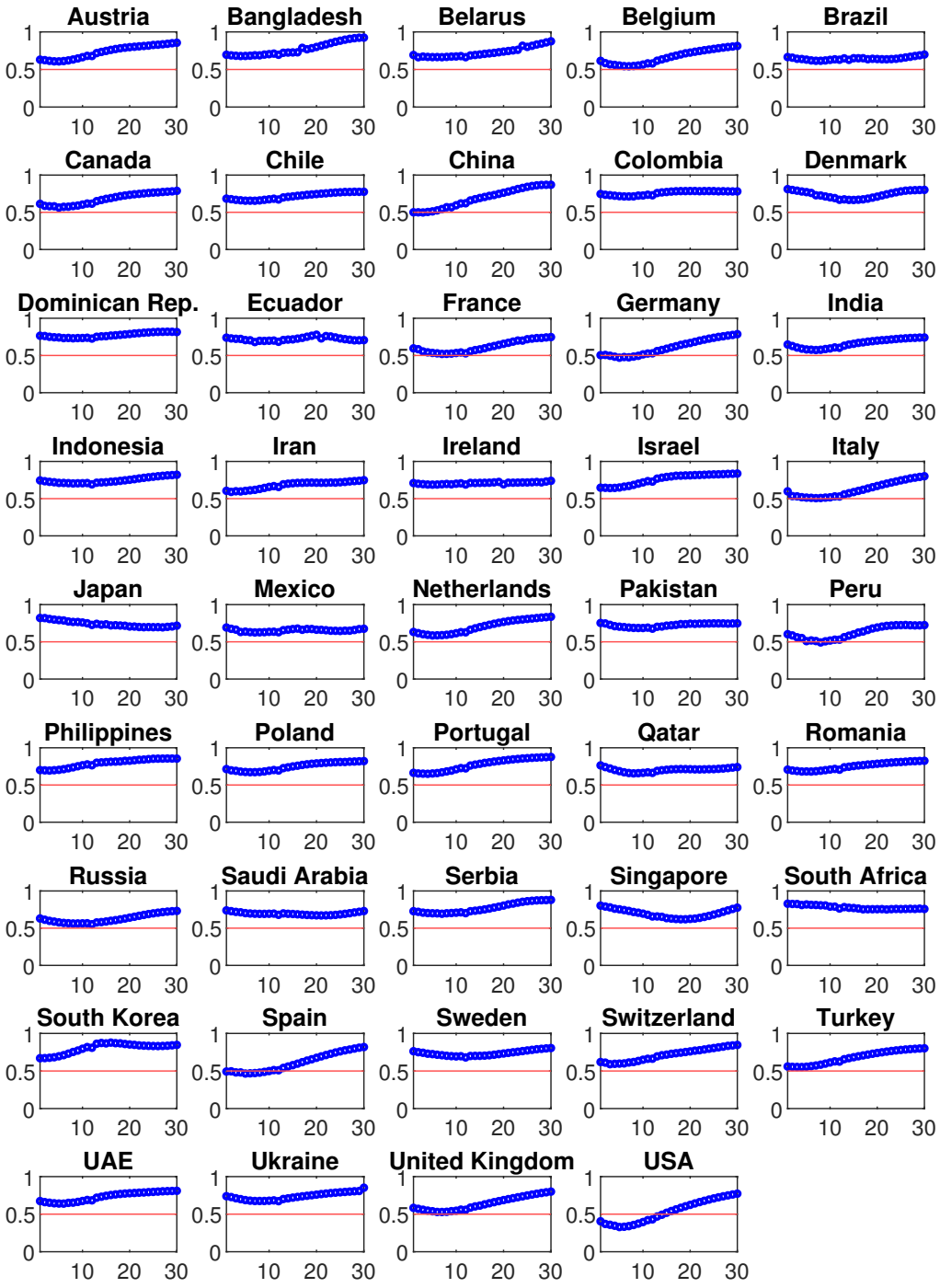

Figure 2: MIDIS: Absolute Values

$(\alpha = 1/7,\ \beta = 0.111,\ \mu = 0.2376,\ d_0^{\mathrm{CHN}} = 0.5)$

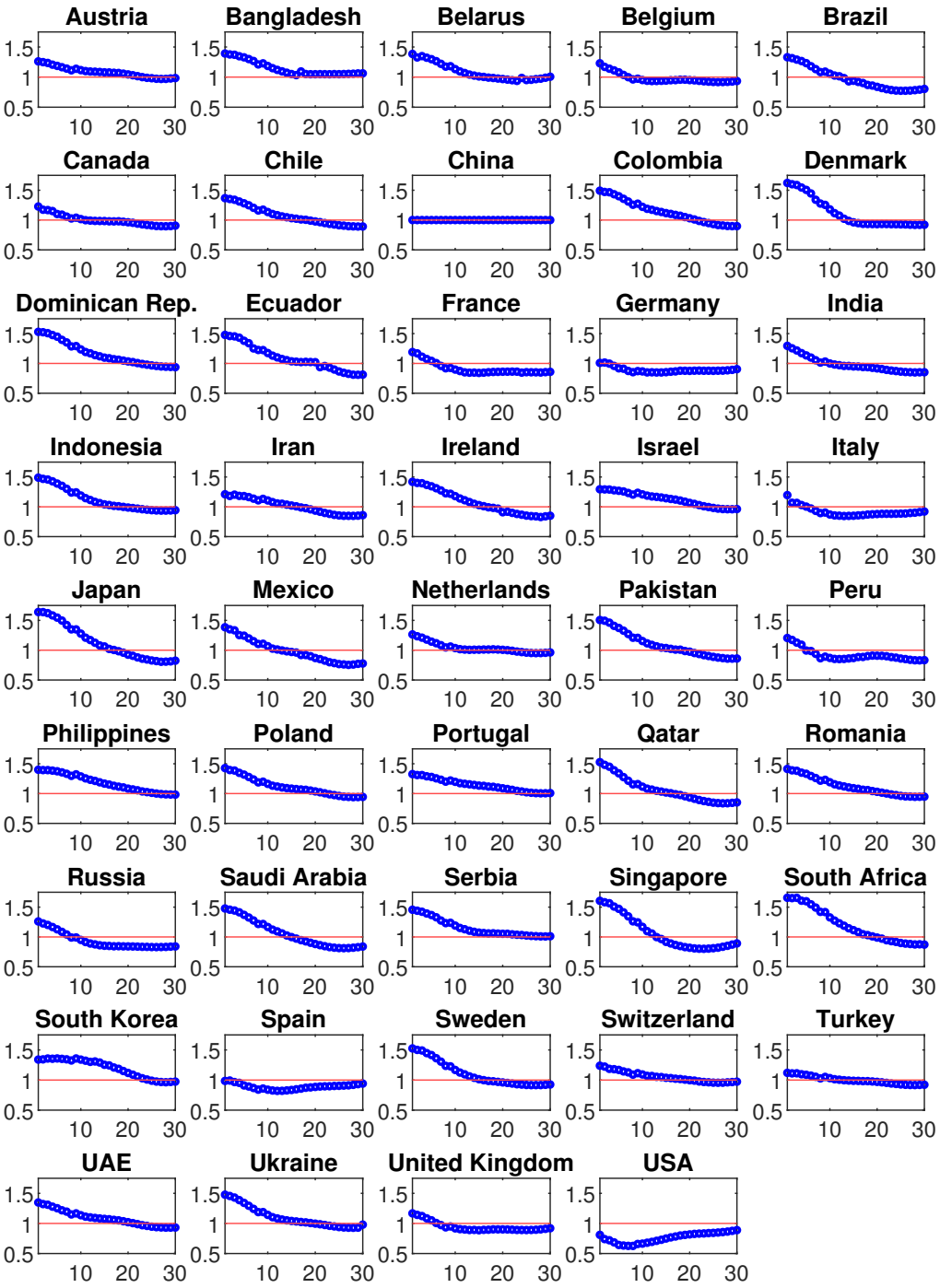

Figure 3: MIDIS: Relative to China

$(\alpha = 1/7,\ \beta = 0.111,\ \mu = 0.2376,\ d_0^{\text{CHN}} = 0.5)$

Table 2: MIDIS: Summary Statistics

Country	init. val.	avg.	std. dev.	max.	min.	acf(1)
South Africa	0.829	0.779	0.027	0.829	0.751	0.884
Japan	0.820	0.739	0.040	0.820	0.694	0.902
Denmark	0.811	0.738	0.050	0.811	0.666	0.908
Singapore	0.803	0.694	0.058	0.803	0.620	0.881
Dominican Rep.	0.765	0.772	0.032	0.819	0.727	0.946
Qatar	0.763	0.703	0.027	0.763	0.656	0.812
Sweden	0.763	0.735	0.036	0.805	0.680	0.897
Pakistan	0.753	0.723	0.025	0.753	0.677	0.900
Colombia	0.746	0.758	0.029	0.786	0.713	0.952
Indonesia	0.745	0.746	0.039	0.820	0.692	0.918
Ecuador	0.739	0.721	0.024	0.779	0.680	0.781
Ukraine	0.739	0.737	0.050	0.852	0.673	0.879
Saudi Arabia	0.739	0.695	0.018	0.739	0.671	0.760
Serbia	0.728	0.771	0.069	0.880	0.693	0.940
Poland	0.714	0.747	0.056	0.821	0.672	0.950
Ireland	0.709	0.709	0.014	0.740	0.688	0.645
Romania	0.707	0.751	0.052	0.825	0.681	0.939
Philippines	0.700	0.790	0.058	0.856	0.694	0.924
Bangladesh	0.696	0.772	0.088	0.924	0.679	0.919
Belarus	0.692	0.728	0.068	0.875	0.663	0.888
Mexico	0.692	0.654	0.018	0.692	0.626	0.721
Chile	0.684	0.716	0.045	0.776	0.655	0.946
UAE	0.674	0.731	0.063	0.810	0.640	0.946
South Korea	0.670	0.803	0.069	0.877	0.670	0.907
Brazil	0.665	0.645	0.020	0.699	0.616	0.746
Portugal	0.663	0.771	0.084	0.877	0.650	0.935
India	0.647	0.660	0.059	0.741	0.573	0.950
Israel	0.647	0.759	0.073	0.837	0.642	0.928
Netherlands	0.632	0.704	0.092	0.837	0.586	0.944
Austria	0.631	0.733	0.089	0.856	0.608	0.935
Russia	0.630	0.626	0.058	0.731	0.553	0.928
Switzerland	0.619	0.713	0.086	0.846	0.590	0.929
Belgium	0.615	0.665	0.095	0.813	0.543	0.943
Canada	0.614	0.677	0.079	0.788	0.564	0.944
Iran	0.605	0.680	0.051	0.748	0.591	0.913
Peru	0.602	0.622	0.086	0.726	0.492	0.957
Italy	0.598	0.623	0.102	0.801	0.507	0.932
France	0.595	0.617	0.080	0.747	0.521	0.940
United Kingdom	0.584	0.641	0.093	0.800	0.529	0.933
Turkey	0.560	0.679	0.091	0.802	0.553	0.932
Germany	0.504	0.609	0.109	0.786	0.470	0.931
China	0.500	0.688	0.133	0.870	0.498	0.926
Spain	0.493	0.611	0.125	0.819	0.466	0.929
USA	0.405	0.533	0.154	0.773	0.329	0.939

Notes: Authors' calculations using the identification methodology explained in Section 3 and the JHU (2020) data. acf(1) is the sample auto-correlation function at one lag.

A pattern observed in a large number of countries features a (minor) decline of MIDIS within the first week that is followed by a persistent (slow) increase later on. Austria, Belgium, France, Germany, India, Italy, Netherlands, Peru, Poland, Russia, Spain, Switzerland, United Arab Emirates, United Kingdom, and the US exhibit such a pattern. For the US, the initial decrease in the first five days of the sample is the fastest in the sample. Hence, the US is not only the country that records the lowest initial MIDIS value; on the sixth day in the sample, the MIDIS value of the US converges to the minimum of the entire sample at 0.332. The maximum MIDIS value for the sixth day is equal to 0.813 and observed in South Africa.

The evolution of MIDIS in countries that attain the highest initial values is notably different. In Japan and South Africa, MIDIS keeps decreasing at a slow rate during the entire sample period. In Denmark and Singapore, however, there is a clear U-shaped pattern where MIDIS takes its lowest values around the middle of the 30-day period.

We observe the most distinguished pattern of MIDIS during the 30-day period in South Korea. Starting at a moderately high value of 0.67, MIDIS in South Korea increases fast and converges to over 0.85 on around the 15th day. In the second half of the episode, the country sustains a high level of MIDIS. In that second half, the average MIDIS value in South Korea is 0.87. The country also attains the highest full-sample average of 0.80 across 44 countries. Table 2 presents a detailed account of MIDIS statistics for all countries.

Figure 3 pictures the evolution of MIDIS relative to China. Some interesting messages follow from this figure as well. The common pattern is a persistent decrease below unity. Decreases are more visible in countries with larger initial MIDIS values, as expected.

In most countries, MIDIS in relative terms stabilizes below or above unity after some time. In countries such as Belgium, France, Germany, Italy, Netherlands, and United Kingdom, this stabilization occurs after 10 days. In other countries such as Bangladesh, Denmark, Russia, and Sweden, stabilization is achieved later.

An interesting observation is that there are only three countries—Bangladesh, Portugal, and Serbia—that record MIDIS values larger than the Chinese level for the entire sample. Hence, if China truly serves as a benchmark for distancing, then only three countries in our sample of 44 countries sustain distancing more effectively than China in the 30-day episode that follow the 500th confirmed case. For the rest, the initial success in distancing is not continued, and MIDIS values decreases below unity somewhere in the second half of the 30-day episode.

We should also underline that two countries with initial MIDIS values less than the Chinese benchmark—Spain and the US—cannot forge ahead China during the sample period. Put differently, relative MIDIS values for these countries remain lower than the Chinese level for all t. The situation is similar for Germany whose MIDIS values decrease below the Chinese level on the third day. Hence, it is fair to state that Spain, Germany, and the US perform least effectively in terms of distancing during the sample period.

Before concluding this section, we investigate whether the daily mobility data from Apple (2020) and Google (2020) validate our distancing measure MIDIS. In Table 3, we document various regression results where MIDIS is the dependent variable and a mobility indicator from Apple (2020) or Google (2020) is the independent variable. In these regressions, we

Table 3: Validating MIDIS through the Mobility Data

Independent Var.	Parameter	Robust S.E.	# of Countries	# of Obs.	R-squared
A-Driving	-0.170***	0.042	35	1,050	0.0711
A-Transit	-0.189***	0.037	18	540	0.0664
A-Walking	-0.148***	0.039	35	1,050	0.0711
G-RetailRecreation	-0.167***	0.036	40	1,200	0.0612
G-GroceryPharmacy	-0.126***	0.037	40	1,200	0.0709
G-Parks	-0.061*	0.032	40	1,200	0.0077
G-TransitStations	-0.206***	0.043	40	1,200	0.0807
G-Workplace	-0.183***	0.043	40	1,200	0.0662
G-Residential	0.354***	0.103	40	1,200	0.0500

Notes: The reported R-squared is the overall R-squared measure. Superscripts ***, **, and * indicate statistical significance at 1%, 5%, and 10%, respectively. See Table B.1 for variable definitions and data sources.

match the calendar dates for each country, and each row presents the results of a separate regression. Clearly, the results we document here cannot be interpreted as a sign of a causal mechanism because both the mobility indicators and MIDIS quantify the very same phenomenon.

The results show that the mobility indicators are strongly correlated with MIDIS and support the validity of our identification strategy. As expected, increased mobility in residential places are positively associated with MIDIS (the last row), and all the other mobility indicators that represent mobility in public places have a strong, inverse relationship with MIDIS. Among the indicators from Apple (2020), we estimate the largest effect for transit stations, and the magnitude of the estimated slope parameter is close to those we obtain for the mobility indicators measured for transit stations and workplace indicators using the Google (2020) data. In absolute value terms and for the nine indicators we focus on, we estimate that the largest effect originates from the mobility in residential areas, and the smallest one from mobility in parks.

5. Cross-Country Heterogeneity in MIDIS

To examine how our social distancing measure varies with a number of country characteristics along governmental, behavioral, and developmental dimensions, we estimate the following regression at the country-day level, (j,t), with each country being j and each day being t:[5]

$$\text{MIDIS}_{j,t} = \phi_0 + \phi_1 G_{j,t-1} + \phi_2 B_{j,t-1} + \phi_3 \mathbf{D}_j + \epsilon_{j,t} \tag{16}$$

Here, $\text{MIDIS}_{j,t}$ is the social distancing measure we construct in this paper at (j,t) level. We rescale this variable to vary between 0 and 100 in regressions. The next two variables are to control for the effect of NPIs on MIDIS: $G_{j,t-1}$ is governmental response to the pandemic,

5 We avoid using time fixed effects in (16) since they were already taken into account in the construction of MIDIS as explained in Section 3.

and $B_{j,t-1}$ is behavioral response to the pandemic by individuals. We use the lagged values of these variables to account for the time-lapse in social distancing as a response to various NPIs. $\mathbf{D}_j$ is a vector of country-specific indicators of comparative development.

First, the data for governmental response are from the Oxford COVID-19 Government Response Tracker (OxCGRT), which collects information on a multitude of containment measures taken by 201 countries and territories around the globe.[6] These measures are school closures, workplace closures, cancellation of public events, bans on public transport, domestic and international travel, government information campaigns, contact tracing and extended testing. All but the last two are used to construct the COVID-19 Government Response Stringency Index, which varies between 0 and 100. We use the lagged values of this index, $stringency_{j,t-1}$, in (16) to proxy for governmental response to the COVID-19 pandemic, $G_{j,t-1}$.

Second, we use JHU (2020) epidemiological data components as proxies for behavioral response to the pandemic. It would not be hard for anyone, who consciously experienced the COVID-19 pandemic, to recall that they had to drop everything to get the news of the numbers of infected, deceased, and recovered for the COVID-19 cases in their cities, countries, and the world every day to prepare for the next day. In other words, people use daily epidemiological data, particularly the numbers of infected or deceased individuals, that headlined all types of news outlets to inform their behavior on the next day. Therefore, we utilize the lagged values of infected and deceased people, $infected_{j,t-1}$ and $deceased_{j,t-1}$, to explore the effect of behavioral response on social distancing.[7] These variables are expressed as the total number in 1,000 population in (16).

Finally, we investigate how social distancing varies with a range of country characteristics borrowed from the comparative development literature to understand the importance of cross-country heterogeneity in geography as well as economic, social, and cultural development (e.g., Easterly and Levine, 1997; Acemoglu et al., 2001; Alesina et al., 2003; Ashraf and Galor, 2013). In particular, we use GDP per capita ($loggdppc_j$), human capital index ($humancap_j$), social progress index (spi_j), ethnolinguistic fractionalization ($ethnofrac_j$), and continent dummies. The definitions and data sources of all the variables used in the regressions are compactly presented in Table B.1, and Table B.2 reports the summary statistics.

Table 4 displays the regression results of different specifications of (16) by progressively adding variables. Column (1) explores the impact of governmental response to the pandemic. The variable $stringency_{j,t-1}$ has a significant positive impact on the level of social distancing. As governments adopt more stringent containment measures, social distancing proliferates. Indeed, a 1 point increase in stringency increases MIDIS by 1/3 of a point.

---

6 A detailed description of the data is provided by Hale et al. (2020) and the dataset is available at `https://covidtracker.bsg.ox.ac.uk`.

7 As in Alfaro et al. (2020), we have also used variables such as "risk taking," "patience," "reciprocity," or "altruism" from the Global Preferences Survey of Falk et al. (2018) and Falk et al. (2016). However, most probably due to very low variation in these variables for our sample of 44 counties, we could not obtain any significant results.

Table 4: Heterogeneity of MIDIS in Different Dimensions

Variables	(1) Governmental	(2) Governmental & Behavioral	(3)	(4)	(5) Governmental, Behavioral & Developmental	(6)	(7)	(8)	(9)	(10) Fixed Effects
$stringency_{j,t-1}$	0.303***			0.177***	0.176***	0.174***	0.174***	0.180***	0.172***	0.169***
	(0.057)			(0.048)	(0.047)	(0.048)	(0.047)	(0.047)	(0.045)	(0.018)
$infected_{j,t-1}$		0.232***								
		(0.070)								
$deceased_{j,t-1}$			3.797***	3.159***	3.165***	3.177***	3.175***	3.144***	3.204***	3.351***
			(0.441)	(0.422)	(0.419)	(0.416)	(0.419)	(0.419)	(0.416)	(0.212)
$humancap_j$					-0.315					
					(1.912)					
spi_j						-0.054				
						(0.088)				
$loggdppc_j$							-1.102			
							(1.027)			
$ethnofrac_j$								-0.088*		
								(0.045)		
$europe_j$									-4.132*	
									(2.212)	
$northamerica_j$									-13.217**	
									(6.506)	
$latinamerica_j$									-3.953	
									(2.573)	
$ssafrica_j$									3.832***	
									(1.472)	
R-squared	0.125	0.025	0.023	0.106	0.106	0.110	0.115	0.145	0.195	0.664
# of Countries	43	44	44	43	43	43	43	43	43	43
# of Obs.	1,247	1,276	1,276	1,247	1,247	1,247	1,247	1,247	1,247	1,247

Notes: The reported R-squared is the overall R-squared measure. Superscripts ***, **, and * indicate statistical significance at 1%, 5%, and 10%, respectively. See Table B.1 for variable definitions and data sources.

Columns (2) and (3) explore behavioral responses only. The former uses the number of people infected whereas the number of deceased due to the COVID19 is utilized in the latter. Both have a positive and significant impact on the level of social distancing. While 1 more infected person in 1,000 population increases MIDIS by 0.23 points, 1 more deceased person among 1,000 increases MIDIS by 3.2 points. Considering the much grimmer impact of the rise in the number of deaths, it is natural to expect a higher behavioral effect from the number of deceased compared to the number of infected. In the remaining specifications, we use $deceased_{j,t-1}$ to gauge for the behavioral response; however, our results with $infected_{j,t-1}$ are qualitatively similar and available upon request. Column (4) reports governmental and behavioral dimensions together, and both parameters stay positive and significant.

In columns (5)-(8), we add the variables $humancap_j$, spi_j, $loggdppc_j$, and $ethnofrac_j$ one by one since these are highly correlated with each other as shown in Table B.3. Except for a barely significant ethnolinguistic fractionalization, none of these variables are significant in explaining MIDIS. Very little cross-country variation in these variables in our 30-day sample with only 44 countries may be the culprit here. However, it may also indicate that the virus—hence social distancing—does not differentiate between developed or otherwise and can manifest itself in unexpected ways compared to our conventional wisdom. When we add continent dummies in column (9), however, it is seen that while the level of social distancing in Europe and North America is lower compared to Asia (the excluded category), it is higher in Sub-Saharan Africa. This is in line with results discussed in Section 4.

Variables measuring governmental and behavioral responses to the COVID-19 pandemic are robustly positive and significant in columns (5)-(9). The last specification reported in the column (10) of Table 4 shows that, even when we use country fixed effects, the effects of governmental and behavioral responses on MIDIS remain to be robust. As expected, the fixed effects model returns a much higher *R-squared* value.

6. MIDIS and Output Loss

This section presents an application for the use of the social distancing measure, MIDIS, constructed in this paper. We focus on the economic costs of social distancing triggered by the COVID-19 pandemic.

Baldwin and Weder di Mauro (2020a) clearly explain the types of economic shocks created by the COVID-19 pandemic that cause reduced economic activity. Among these, we concentrate on output loss. Following these authors' general guidelines, we can say that, on the one hand, even with no response at all to the pandemic, there is output loss due to sick people not being able to produce (a medical shock). On the other hand, social distancing caused by governmental and behavioral responses to the pandemic creates distances between workers and work as well as consumers and consumption, which results in further output losses.

The link between output loss and social distancing can best be explained by the help of a diagram that is now familiar to many. Figure 4 shows the epidemiological curves—bell shaped curves of the number of new cases over time—with (blue) and without (red) social

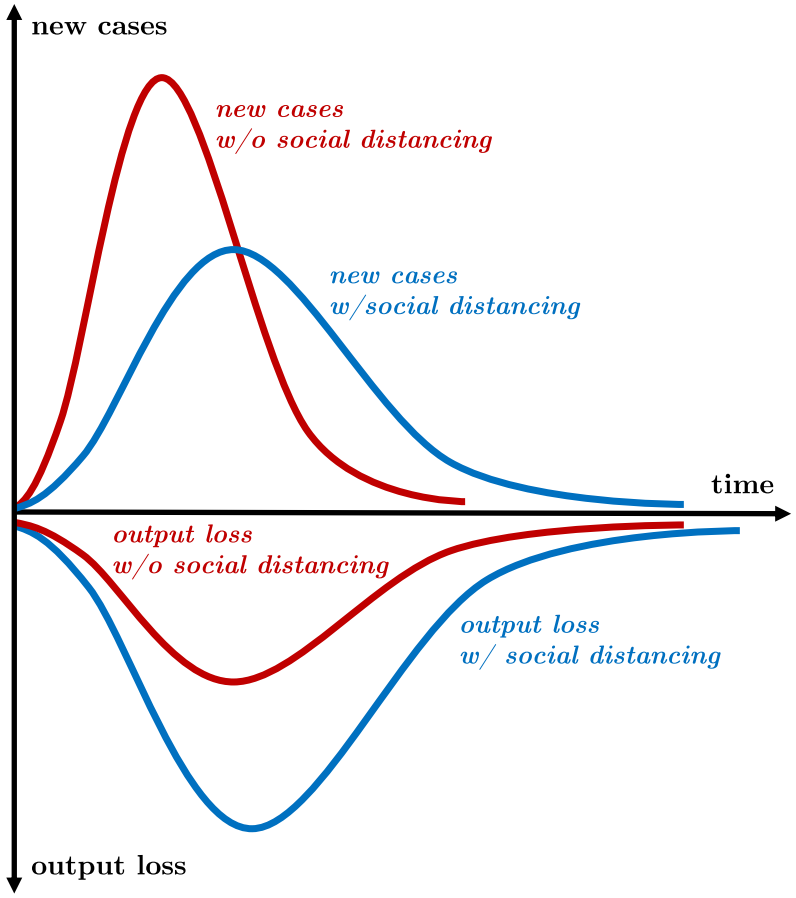

Figure 4: Social Distancing, Epidemiological Curve and Output Loss

Source: Authors' elaboration, inspired by Baldwin and Weder di Mauro's (2020b) illustration

distancing in the top panel, and the corresponding output loss curves in the bottom panel.

Considering the fact that COVID-19 is an extremely infectious killer that causes higher death rates when the patients are not well cared for, it is obvious that social distancing does not directly save people from dying but saves their lives by preventing congestion in healthcare facilities. So, the top panel of Figure 4 implies that COVID-19 kills many people, but it kills less with social distancing. This is what is meant by "flattening the curve" by epidemiologists. The bottom panel, however, illustrates that existence and/or stringency of social distancing measures proliferates output losses during a pandemic (Gourinchas, 2020).

Even though in our subsequent analysis we choose to stay oblivious to the exact channels of output loss during the COVID-19 pandemic, it is important to briefly mention them here for the sake of argument. There are demand and supply side components of output loss experienced during the pandemic. The main channels of demand disruptions are (i)

a direct hit to aggregate demand components due to the medical shock as well as social distancing and (ii) an expectation shock to consumption and investment due to wait-and-see type delays by consumers and firms. The main channels of supply disruptions are (i) a direct hit to aggregate supply through reduced production capability resulting from the medical shock as well as social distancing and (ii) a supply-chain contagion as the disease jumps from one country to the other against the background of internationally fragmented production structure across the globe.

6.1. Proxying for Output Loss

Unlike epidemiological data, it is impossible to come by daily data for output, which makes using a proxy instead a necessity. Therefore, we use the Bruegel Electricity Tracker (BET) of COVID-19 Lockdown Effects compiled and calculated by McWilliams and Zachmann (2020) to approximate output loss experienced during the pandemic based on the premise that much economic activity heavily relies on the use of electricity. BET reports the temperature-adjusted daily sums of peak-hour electricity consumption (08:00-18:00) as a measure of economic activity owing to the intensity of economic activity within these hours. BET sample spanned 20 countries[8] between March 4-May 13, 2020 in the time of writing this paper.[9]

Let relative output be the ratio of daily peak-hour electricity consumption in 2020 to that in 2019 and state it as a percentage:

$$\text{relative output}_{j,t} = \left(\frac{\text{output}_{j,t}^{2020}}{\text{output}_{j,t}^{2019}} \right) \times 100 \tag{17}$$

Here, we calculate relative output for country j on day t by aligning each week in 2020 with the corresponding week in 2019. In our analysis, we include only working days (ignoring weekends and public holidays from our sample of 30 days for which MIDIS is calculated), which leaves us with 20-22 days for each country.

Figure 5 illustrates the evolution of relative output (blue points) and MIDIS (black points) in these 30 days along with a hypothetical red line that shows the case of no output loss by crossing the vertical axis at the value of 100.

The first observation from Figure 5 is that, with the exceptions of Denmark, Japan, and Sweden, all countries experienced a visible decline in their output levels relative to 2019. For many countries in the sample, there is output loss either for the entirety or the majority of the days considered. In Austria, India, Netherlands, Poland, and Switzerland, for instance, relative output is less than 100 percent for all the days in their respective samples.

The closer inspection of Figure 5 also reveals that there might exist a scale effect from MIDIS to relative output in the sense that output losses remain minuscule as long as MIDIS remains sufficiently low. The cases of the US, Spain, Germany, and Italy—and of the UK to

8 Austria, Belgium, Denmark, France, Germany, India, Ireland, Italy, Japan, Netherlands, Poland, Portugal, Romania, Serbia, Spain, Sweden, Switzerland, Ukraine, the UK and the US.

9 A detailed description of the temperature adjustment methodology is provided at the Bruegel website.

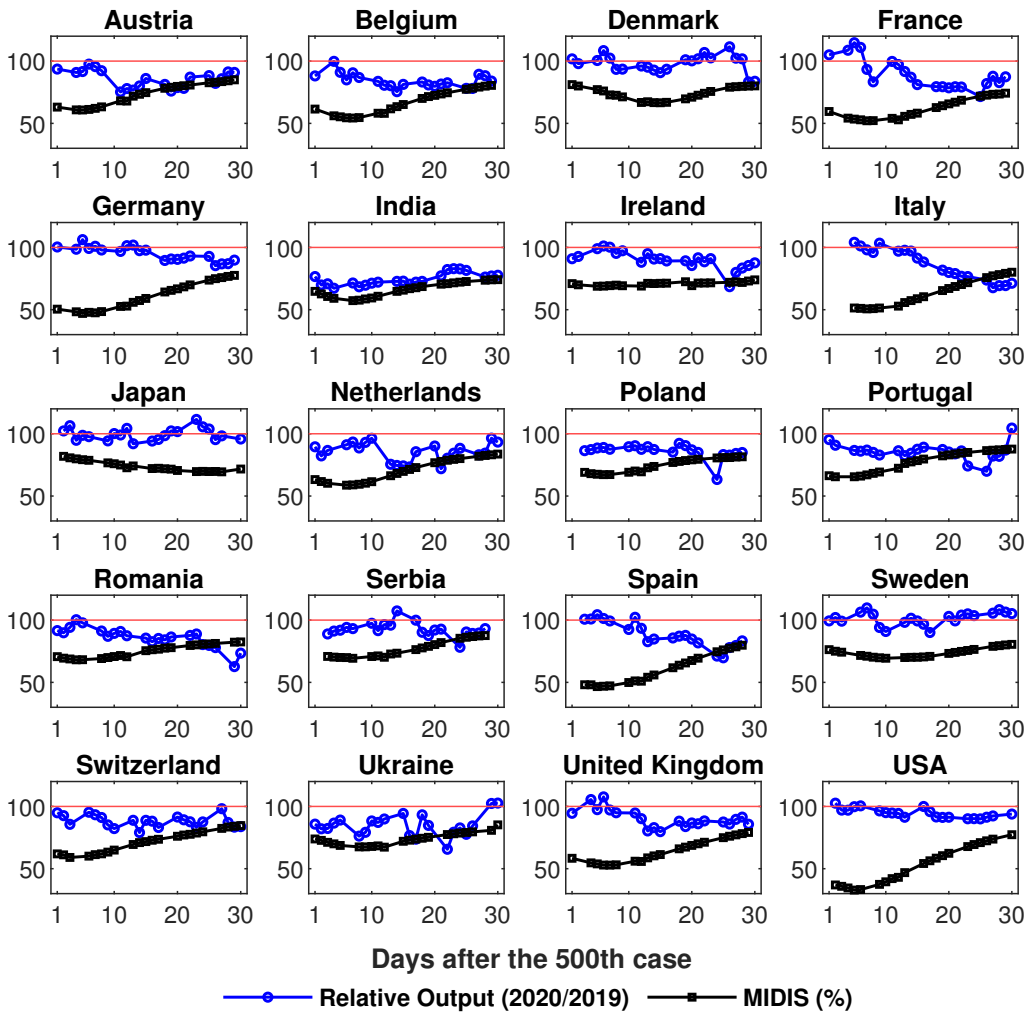

Figure 5: MIDIS and Relative Output

a lesser extent—suggest that countries that enter the 30-day episode with a MIDIS level less than or very close to 50 percent do not face (sizable) drops in relative output. In all of these countries, the decline of relative output seems to have required sufficiently large increases in MIDIS after a particular date.

Figure 5 also shows that the relationship between MIDIS and relative output is not uniform across countries and days. Some countries such as France, Italy, and Spain exemplify the strong negative association, but the relationship turns out be less visible in some countries after a particular date. For instance, in Austria, there seems to be a counterintuitively positive association between relative output and MIDIS after the 10th day. The same is true for Spain for the fourth quarter of the 30-day episode. In some countries, the continuing increase in MIDIS within a particular episode is observed along with a trendless movement

Table 5: MIDIS and Output Loss

	Weekends Excluded			Weekends & Holidays Excluded		
MIDIS	0.228***	0.377***	0.315***	0.216***	0.366***	0.356***
	(0.039)	(0.041)	(0.068)	(0.038)	(0.040)	(0.065)
Country FE	No	Yes	Yes	No	Yes	Yes
Time FE	No	No	Yes	No	No	Yes
R-squared	0.062	0.525	0.585	0.058	0.570	0.633
# of Countries	20	20	20	20	20	20
# of Obs.	425	425	425	407	407	407

Notes: The reported R-squared is the adjusted R-squared measure. Superscripts ***, **, and * indicate statistical significance at 1%, 5%, and 10%, respectively. See Table B.1 for variable definitions and data sources.

of relative output. In Belgium after the 10th day, for instance, MIDIS increases from around 50 percent to 80 percent but relative output fluctuates within the proximity of 80 percent.

We observe an example of non-uniformity from the other direction as well. In Ireland, the trendless movement of MIDIS within the neighborhood of 70 percent for the entire episode is accompanied by successive episodes of slow increase, slow decrease, stability, sharp decrease, and sharp increase.

Overall, however, there exists a moderately strong, inverse relationship between MIDIS and relative output. For each country, the correlation coefficient is negative. These correlation coefficients range between -0.19 and -0.73, with an average of -0.34, and all of them are statistically significant at 5 percent confidence level.

6.2. Estimation Results

To explore the relationship between social distancing and output loss, we estimate a very basic regression specification at the country-day level, (j, t), with each country being j and each day being t:

$$\text{output loss}_{j,t} = \phi \text{MIDIS}_{j,t} + \mu_j + \delta_t + \epsilon_{j,t} \tag{18}$$

where $\text{output loss}_{j,t} = 100 - \text{relative output}_{j,t}$, and μ_j and δ_t denote country and day fixed effects, respectively. Here, ϕ can be interpreted as the social distancing elasticity of output loss given that both MIDIS and output loss are expressed in percentages.

Table 5 reports the estimation results for (18) using different fixed effects structures. The left panel is for the sample excluding weekends and the right panel for the sample excluding both weekends and public holidays. The results indicate a robust positive impact of MIDIS on output loss. In other words, an escalation in social distancing increases output loss. Indeed, the social distancing elasticity of output loss vary between 0.22 and 0.38 depending on the specification. Put it another way, a 10 percent increase in social distancing causes 2.2-3.8 percent increase in output loss, which is large in any account.

In short, the social distancing measure implied by the SEIRD model and daily epidemiological data explains output losses experienced during the COVID-19 pandemic in a

meaningful way. Clearly, the effects of MIDIS on output loss that we document in Table 5 do not identify the structural mechanisms, but the regression serves as a reduced-form device that allows us to see the quantifiable output impact of distancing.[10]

7. Concluding Remarks

In this paper, we make a first attempt to identify a social distancing term for each country and each day within the framework of the SEIRD model to be able to construct a distancing measure with minimum data requirements. This is critical in the context of the current COVID-19 pandemic because until a vaccine or an effective antiviral treatment is developed, policymakers as well as individuals will be in the midst of the tension between *necessity* and *tolerability* of social distancing. On the one hand, there is a need to sufficiently contain the spread of the disease through social distancing to prevent an overrun on the healthcare facilities. On the other hand, it will be impossible to continue social distancing—either through governmental or individual measures—indefinitely, since people's livelihoods depend on being able to work. As a result, to inform their decision making process, it would be desirable for policymakers as well as individuals to have access to a relatively reliable and robust distancing measure with a minimum requirement of high-frequency data. The social distancing term we identify in this paper (MIDIS) may be a candidate for that role.

When we take MIDIS to data, our results successfully exhibit the cross-country and over-time heterogeneity in social distancing during the COVID-19 pandemic. We also show that MIDIS is highly correlated with the mobility data, and it embeds both governmental and behavioral responses to the pandemic. Furthermore, when we use MIDIS to explain output losses experienced during the pandemic, we are able to show a robust positive correlation between the two—with sizable economic effects.

In sum, we consider our paper as an initial attempt to improve the SEIRD model and a contribution to the intense debate on the effects of the COVID-19 pandemic. We expect our qualitative results to be informative and useful. However, due to the highly stylized nature of the underlying epidemiological model we use to construct MIDIS, we urge our readers to interpret our quantitative results with care. Since the world governments are taking steps in easing lockdown restrictions in the time of writing this paper, we can safely say that there is much to change in the near future in regards to social distancing and its diverse effects on the lives of people. Our hope is to continue this line of work to incorporate what we miss in the current version and the new developments in the pandemic as they arise.

10 The strong relationship between distancing and output loss is expected to hold in the very short run, e.g., a month, and it may weaken and be reversed in the longer run. This is because both the centralized/optimal distancing policies and decentralized/individual distancing practices are time-dependent—changing daily—as demonstrated in the related literature (Bethune and Korinek, 2020; Farboodi et al., 2020). We thank an anonymous reviewer for pointing this out.

References

Acemoglu, D., V. Chernozhukov, I. Werning, and M. D. Whinston (2020): "Optimal Targeted Lockdowns in a Multi-Group SIR Model," Working Paper 27102, National Bureau of Economic Research, 10.3386/w27102.

Acemoglu, D., S. Johnson, and J. A. Robinson (2001): "The Colonial Origins of Comparative Development: An Empirical Investigation," *American Economic Review*, 91 (5), 1369–1401.

Alesina, A., A. Devleeschauwer, W. Easterly, S. Kurlat, and R. Wacziarg (2003): "Fractionalization," *Journal of Economic growth*, 8 (2), 155–194.

Alfaro, L., E. Faia, N. Lamersdorf, and F. Saidi (2020): "Social Interactions in Pandemics: Fear, Altruism, and Reciprocity," Working Paper 27134, National Bureau of Economic Research, 10.3386/w27134.

Alvarez, F. E., D. Argente, and F. Lippi (2020): "A Simple Planning Problem for COVID-19 Lockdown," *Covid Economics: Vetted and Real-Time Papers* (14).

Apple (2020): "Mobility Trends Reports," https://www.apple.com/covid19/mobility.

Argentieri Mariani, L., J. Gagete-Miranda, and P. Rettl (2020): "Words can hurt: How political communication can change the pace of an epidemic," *Covid Economics: Vetted and Real-Time Papers*, 1 (12).

Ashraf, Q., and O. Galor (2013): "The 'Out of Africa' Hypothesis, Human Genetic Diversity, and Comparative Economic Development," *American Economic Review*, 103 (1), 1–46.

Askitas, N., K. Tatsiramos, and B. Verheyden (2020): "Lockdown strategies, mobility patterns and Covid-19," *Covid Economics: Vetted and Real-Time Papers*, 1 (23).

Avery, C., W. Bossert, A. T. Clark, G. Ellison, and S. F. Ellison (2020): "Policy implications of models of the spread of coronavirus: Perspectives and opportunities for economists," *Covid Economics: Vetted and Real-Time Papers*, 1 (12).

Baldwin, R., and B. Weder di Mauro (2020a): *Economics in the Time of COVID-19*, VoxEU.org Book, London: Centre for Economic Policy Research.

——— (2020b): *Mitigating the COVID economic crisis: Act fast and do whatever it takes*, VoxEU.org Book, London: Centre for Economic Policy Research.

Berger, D. W., K. F. Herkenhoff, and S. Mongey (2020): "An SEIR Infectious Disease Model with Testing and Conditional Quarantine," Working Paper 26901, National Bureau of Economic Research, 10.3386/w26901.

Bethune, Z., and A. Korinek (2020): "COVID-19 infection externalities: Pursuing herd immunity or containment?" *Covid Economics: Vetted and Real-Time Papers*, 1 (11).

Brzezinski, A., G. Deiana, V. Kecht, and D. V. Dijcke (2020): "Government versus community action across the United States," *Covid Economics: Vetted and Real-Time Papers*, 1 (7).

Castex, G., E. Dechter, and M. Lorca (2020): "COVID-19: Cross-country heterogeneity in effectiveness of non-pharmaceutical interventions," *Covid Economics: Vetted and Real-Time Papers*, 1 (14).

Chang, R., and A. Velasco (2020): "Economic policy incentives to preserve lives and livelihoods," *Covid Economics: Vetted and Real-Time Papers*, 1 (14).

Chen, X., and Z. Qiu (2020): "Scenario analysis of non-pharmaceutical interventions on global Covid-19 transmissions," *Covid Economics: Vetted and Real-Time Papers*, 1 (7).

Chowell, G., P. W. Fenimore, M. A. Castillo-Garsow, and C. Castillo-Chavez (2003): "SARS outbreaks in Ontario, Hong Kong and Singapore: the role of diagnosis and isolation as a control mechanism," *Journal of Theoretical Biology*, 224 (1), 1–8, 10.1016/s0022-5193(03)00228-5.

Chudik, A., M. H. Pesaran, and A. Rebucci (2020): "Voluntary and mandatory social distancing: Evidence on Covid-19 exposure rates from Chinese provinces and selected countries," *Covid Economics: Vetted and Real-Time Papers*, 1 (15).

Cochrane, J. H. (2020): "An SIR Model with Behavior," https://johnhcochrane.blogspot.com/2020/05/an-sir-model-with-behavior.html, The Grumpy Economist Blog.

Coven, J., and A. Gupta (2020): "Disparities in Mobility Responses to COVID-19,"Technical report, NYU Stern Working Paper.

Deb, P., D. Furceri, J. D. Ostry, , and N. Tawk (2020): "The effect of containment measures on the COVID-19 pandemic," *Covid Economics: Vetted and Real-Time Papers*, 1 (19).

Degue, K. H., and J. Le Ny (2018): "An Interval Observer for Discrete-Time SEIR Epidemic Models," in *2018 Annual American Control Conference (ACC)*, 5934–5939.

Doganoglu, T., and E. Ozdenoren (2020): "Should I stay or should I go (out): The role of trust and norms in disease prevention during pandemics," *Covid Economics: Vetted and Real-Time Papers*, 1 (16).

Drazanova, L. (2019): "Historical Index of Ethnic Fractionalization Dataset (HIEF)," 10.7910/DVN/4JQRCL.

Durante, R., L. Guiso, and G. Gulino (2020): "Civic Capital and Social Distancing: Evidence from Italians' Response to COVID-19," *VoxEU Column*.

Easterly, W., and R. Levine (1997): "Africa's growth tragedy: policies and ethnic divisions," *Quarterly Journal of Economics*, 112 (4), 1203–1250.

Eichenbaum, M. S., S. Rebelo, and M. Trabandt (2020): "The Macroeconomics of Epidemics," Working Paper 26882, National Bureau of Economic Research, 10.3386/w26882.

Engle, S., J. Stromme, and A. Zhou (2020): "Staying at home: Mobility effects of Covid-19," *Covid Economics: Vetted and Real-Time Papers*, 1 (4).

Falk, A., A. Becker, T. Dohmen, B. Enke, D. Huffman, and U. Sunde (2018): "Global evidence on economic preferences," *Quarterly Journal of Economics*, 133 (4), 1645–1692.

Falk, A., A. Becker, T. J. Dohmen, D. Huffman, and U. Sunde (2016): "The preference survey module: A validated instrument for measuring risk, time, and social preferences," IZA Discussion Paper No. 9674 https://github.com/CSSEGISandData/COVID-19.

Farboodi, M., G. Jarosch, and R. Shimer (2020): "Internal and external effects of social distancing in a pandemics," *Covid Economics: Vetted and Real-Time Papers*, 1 (9).

Feenstra, R. C., R. Inklaar, and M. P. Timmer (2015): "The Next Generation of the Penn World Table," *American Economic Review*, 105 (10), 3150–82, 10.1257/aer.20130954.

Feng, Z. (2007): "Final and peak epidemic sizes for SEIR models with quarantine and isolation," *Mathematical Biosciences & Engineering*, 4 (4), 675–686.

Fernández-Villaverde, J., and C. I. Jones (2020): "Estimating and Simulating a SIRD Model of COVID-19 for Many Countries, States, and Cities,"Technical report, National Bureau of Economic Research.

Google (2020): "COVID-19 Community Mobility Results," https://www.google.com/covid19/mobility/.

Gourinchas, P.-O. (2020): "Flattening the Pandemic and Recession Curves," in *Mitigating the COVID economic crisis: Act fast and do whatever it takes* ed. by Baldwin, R., and Weder di Mauro, B. London: Centre for Economic Policy Research, 31–40.

Hale, T., N. Angrist, B. Kira, A. Petherick, T. Phillips, and S. Webster (2020): "Variation in government responses to COVID-19," BSG Working Paper Series 2020/032, https://www.bsg.ox.ac.uk/research/research-projects/coronavirus-government-response-tracker.

He, S., S. Tang, and L. Rong (2020): "A Discrete Stochastic Model of the COVID-19 Outbreak: Forecast and Control," *Mathematical Biosciences and Engineering*, 17 (4), 2792–2804.

JHU (2020): "COVID-19 Data Repository," https://github.com/CSSEGISandData/COVID-19.

Kaplan, G., B. Moll, and G. Violante (2020): "Pandemics According to HANK," https://benjaminmoll.com/wp-content/uploads/2020/03/HANK_pandemic.pdf.

Kermack, W. O., and A. G. McKendrick (1927): "A Contribution to the Mathematical Theory of Epidemics," *Proceedings of the Royal Society of London. Series A, Containing Papers of a Mathematical and Physical Character*, 115 (772), 700–721.

Kmenta, J. (1991): "Latent Variables in Econometrics," *Statistica Neerlandica*, 45 (2), 73–84.

Lekone, P. E., and B. F. Finkenstädt (2006): "Statistical inference in a stochastic epidemic SEIR model with control intervention: Ebola as a case study," *Biometrics*, 62 (4), 1170–1177, 10.1111/j.1541-0420.2006.00609.x.

Maloney, W., and T. Taskin (2020): "Determinants of social distancing and economic activity during COVID-19: A global view," *Covid Economics: Vetted and Real-Time Papers*, 1 (13).

McWilliams, B., and G. Zachmann (2020): "Bruegel electricity tracker of COVID-19 lockdown effects," https://www.bruegel.org/publications/datasets/bruegel-electricity-tracker-of-covid-19-lockdown-effects/, Bruegel Datasets.

Painter, M. O., and T. Qiu (2020): "Political beliefs affect compliance with Covid-19 social distancing orders," *Covid Economics: Vetted and Real-Time Papers*, 1 (4).

SPI (2019): "Social Progress Index," https://www.socialprogress.org/, Social Progress Imperative.

Tang, B., X. Wang, Q. Li, N. L. Bragazzi, S. Tang, Y. Xiao, and J. Wu (2020): "Estimation of the Transmission Risk of the 2019-nCoV and Its Implication for Public Health Interventions," *Journal of Clinical Medicine*, 9(2) (462), 1–13.

Toxvaerd, F. (2020): "Equilibrium Social Distancing," *Covid Economics: Vetted and Real-Time Papers*, 1 (15).

World Bank (2020): "World Development Indicators," https://databank.worldbank.org/source/world-development-indicators.

Zhou, Y., Z. Ma, and F. Brauer (2004): "A discrete epidemic model for SARS transmission and control in China," *Mathematical and Computer Modelling*, 40 (13), 1491 – 1506, https://doi.org/10.1016/j.mcm.2005.01.007.

Appendix A. MIDIS under Alternative Parameter Values

In this appendix, we investigate whether and to what extent the distancing measure MIDIS we identify is sensitive to the parameter values adopted for the benchmark results. We present results for China, South Korea, and the US for space considerations. We choose to focus on South Korea and the US since these are the countries with the highest and lowest average MIDIS values, respectively. The full set of sensitivity results are available upon request.

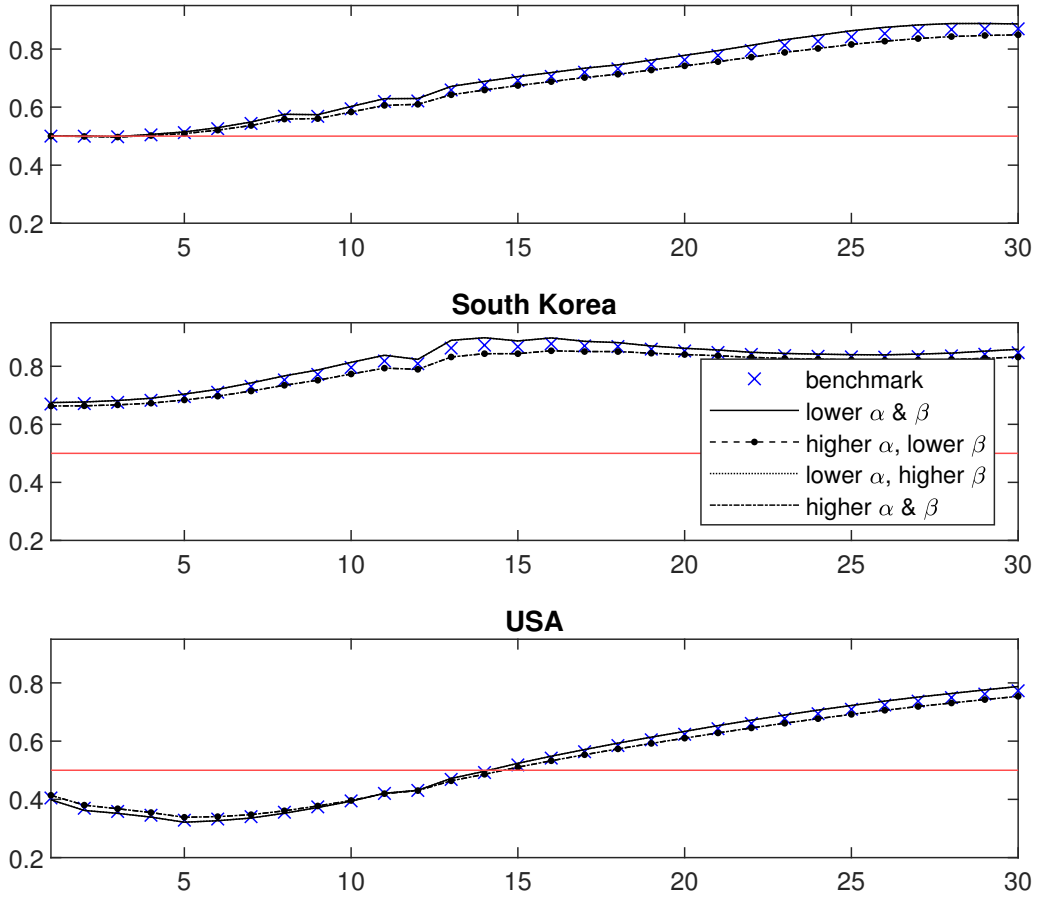

Figure A.1: MIDIS under Alternative (α, β) Values: μ is re-calibrated

Notes: This figure pictures the evolution of MIDIS for China, South Korea, and the US under alternative values of α and β and with a re-calibrated value of μ in each case. For α, the lower and higher values are 1/9 and 1/5, respectively. These correspond to 9 and 5 days of incubation. For β, the lower and higher values are $\beta - 2\hat{\sigma}_\beta = 0.1080$ and $\beta + 2\hat{\sigma}_\beta = 0.1140$, respectively, where $\hat{\sigma}_\beta = 0.0015$ as estimated by He et al. (2020).

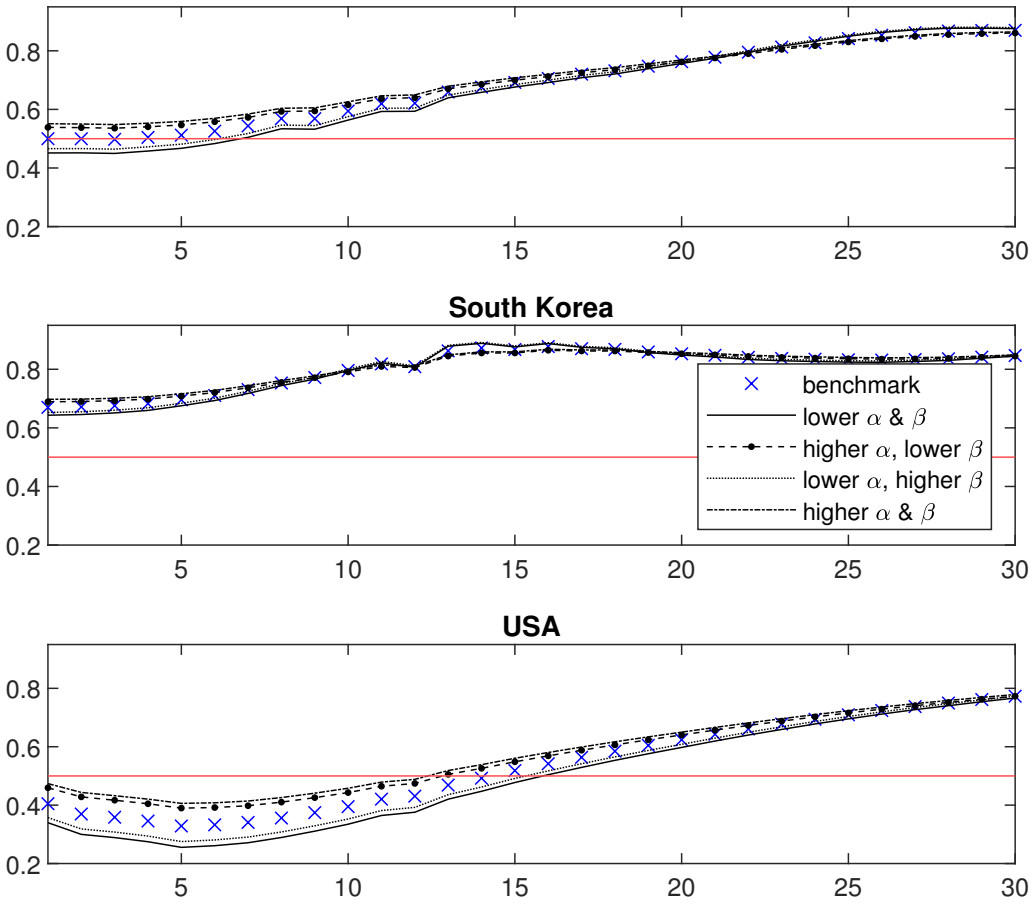

Figure A.2: MIDIS under Alternative (α, β) Values: μ is not re-calibrated

Notes: This figure pictures the evolution of MIDIS for China, South Korea, and the US under alternative values of α and β. For α, the lower and higher values are 1/9 and 1/5, respectively. These correspond to 9 and 5 days of incubation. For β, the lower and higher values are $\beta - 2\hat{\sigma}_\beta = 0.1080$ and $\beta + 2\hat{\sigma}_\beta = 0.1140$, respectively, where $\beta = 0.111$ is the benchmark value, and $\hat{\sigma}_\beta = 0.0015$ is the standard error, both being estimated by He et al. (2020).

Recall that the model has three parameters; β as the pure probability of transmission, α as the inverse of average incubation period, and μ as a free parameter that we adjust by normalizing the initial MIDIS value of China to $d_0^{\text{CHN}} = 0.5$. The benchmark values of these parameters are $\beta = 0.111$, $\alpha = 1/7$, and $\mu = 0.2376$.

For all the scenarios we consider here, we set lower and higher values for both α and β. For the former, the lower value is characterized by 9 days of incubation, and the higher value by 5 days. For the latter, we use the standard error estimated by He et al. (2020) in assigning the lower and higher values to β. Specifically, with the estimated benchmark value of $\beta = 0.111$ and the estimated standard error of $\hat{\sigma}_\beta = 0.0015$, we assign the lower and higher values by constructing a confidence band of 2 standard errors, i.e., $\beta - 2\hat{\sigma}_\beta = 0.1080$ and $\beta + 2\hat{\sigma}_\beta = 0.1140$.

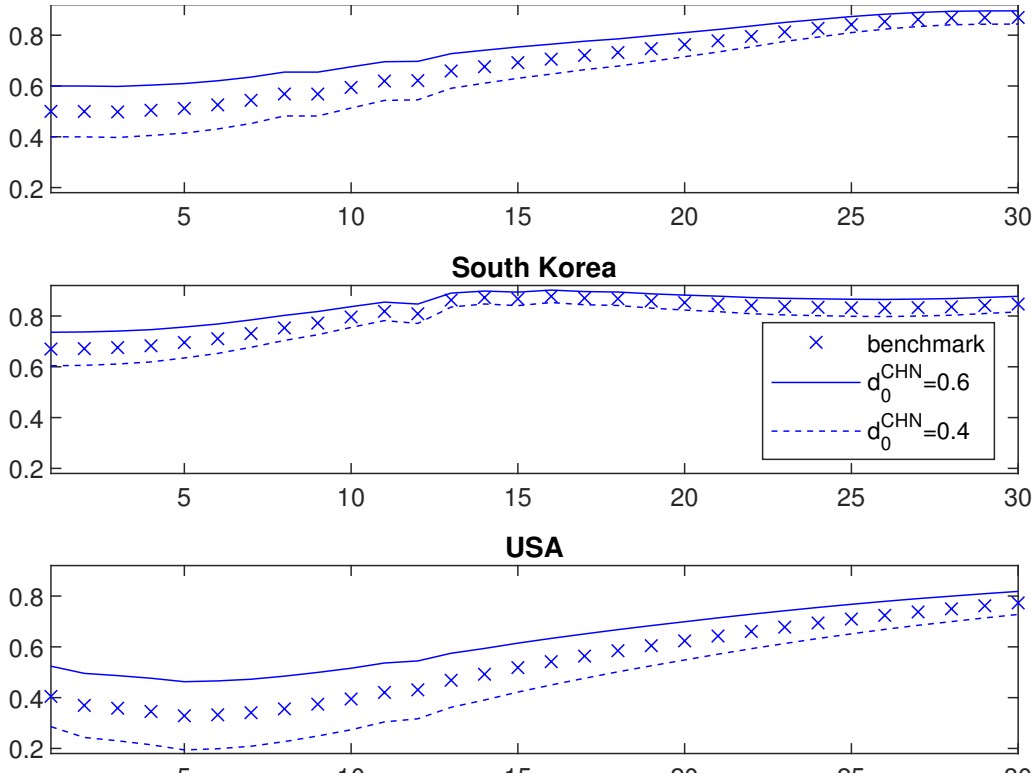

Figure A.3: MIDIS under Alternative d_0^{CHN} Values

Notes: This figure pictures the evolution of MIDIS for China, South Korea, and the US under alternative values of the normalized initial value for China, i.e., $d_0^{\text{CHN}} = 0.5$. Hence, the figure re-calibrates μ for each of the cases. For $d_0^{\text{CHN}} = 0.4$, the re-calibrated value is $\mu = 0.2851$, and, for $d_0^{\text{CHN}} = 0.6$, it is equal to $\mu = 0.19005$.

In the first stage of the sensitivity analysis, we run the algorithm for four different scenarios:

- $\alpha = 1/9$ and $\beta = 0.1080$
- $\alpha = 1/5$ and $\beta = 0.1080$
- $\alpha = 1/9$ and $\beta = 0.1140$
- $\alpha = 1/5$ and $\beta = 0.1140$

Figures A.1 and A.2 picture the results of these scenarios under two sub-scenarios. In the former, we re-calibrate μ to normalize the initial MIDIS value of China to $d_0^{\text{CHN}} = 0.5$ as in the benchmark case. These re-calibrated values are $\mu_1 = 0.21645$, $\mu_2 = 0.25750$, $\mu_3 = 0.22239$, and $\mu_4 = 0.26455$, respectively. In Figure A.2, however, we allow d_0^{CHN} to be different from 0.5 by keeping μ at its benchmark value of $\mu = 0.2376$.

Both figures show that the evolution of MIDIS is not much sensitive to the changes in parameter values. In fact, when we re-calibrate μ, this sterilizes the effect of changes in β, and only the value of α matter for the evolution of MIDIS.

Inspecting Figure A.2 also reveals that the separate effects of α and β on the magnitude of MIDIS for any t are closer to each other in size, but the effect of α is slightly larger.

In the second stage of sensitivity analysis, we investigate whether the normalized MIDIS value for China at $t = 0$ has an effect on the identified MIDIS sequences. In this exercise, we keep α and β at their benchmark levels, but change the target level of d_0^{CHN} and re-calibrate μ. The resulting values of μ for $d_0^{\text{CHN}} = 0.4$ and $d_0^{\text{CHN}} = 0.6$ are $\mu_5 = 0.2851$ and $\mu_5 = 0.19005$, respectively.

Figure A.3 pictures the associated MIDIS values along with the benchmark sequence. Once again, the evolution of MIDIS for the selected countries are qualitatively similar with that of the benchmark. For the three countries considered here, effects are symmetric with respect to the benchmark, and largest for the US and smallest for South Korea.

Appendix B. Statistical Appendix

Table B.1: Variable Definitions and Data Sources

Variable	Definition *Source*
stringency	Stringency Index, score, (0-100) a composite of various government responses *Source*: Hale et al. (2020)
infected	Total number of confirmed COVID-19 cases
deceased	Total number of individuals deceased because of COVID-19 number in 1,000 population *Source*: JHU (2020)
humancap	Human Capital per person, indexed, 2017 values based on years of schooling & returns to education *Source*: Feenstra et al. (2015)
spi	Social Progress Index, score, (0-100) based on more than 50 development indicators *Source*: SPI (2019)
gdppc	GDP per capita, 2018 values purchasing power parity, constant 2017 international dollars *Source*: World Bank (2020)
ethnofrac	Ethnolinguistic Fractionalization, score, (0-100) probability that two randomly drawn individuals within a country are not from the same ethnic group *Source*: Drazanova (2019)
A-Driving	Map requests for driving route directions (relative to Jan 13, 2020, %)
A-Transit	Map requests for transit directions (relative to Jan 13, 2020, %)
A-Walking	Map requests for walking route directions (relative to Jan 13, 2020, %) *Source*: Apple (2020)
G-RetailRecreation	Mobility trends for places like restaurants, cafes, shopping centers, theme parks, museums, libraries, and movie theaters (relative to Jan 3-Feb 6, 2020, %)
G-GroceryPharmacy	Mobility trends for places like grocery markets, food warehouses, farmers markets, specialty food shops, drug stores, and pharmacies (relative to Jan 3-Feb 6, 2020, %)
G-Parks	Mobility trends for places like local parks, national parks, public beaches, marinas, dog parks, plazas, and public gardens (relative to Jan 3-Feb 6, 2020, %)
G-TransitStations	Mobility trends for places like public transport hubs such as subway, bus, and train stations (relative to Jan 3-Feb 6, 2020, %)
G-Workplace	Mobility trends for places of work (relative to Jan 3-Feb 6, 2020, %)
G-Residential	Mobility trends for places of residence (relative to Jan 3-Feb 6, 2020, %) *Source*: Google (2020)
Relative Output	Peak-hour daily electricity consumption in 2020 (relative to 2019 values, %, excluding weekends and holidays) *Source*: McWilliams and Zachmann (2020)

Table B.2: Summary Statistics

Variable	# of Obs.	# of Countries	mean	std. dev.	min	max
MIDIS (%)	1,320	44	70.39	9.17	32.85	92.34
stringency	1,290	43	78.75	17.32	14.29	97.14
infected (in 1,000)	1,320	44	11.98	26.65	0.50	366.32
deceased (in 1,000)	1,320	44	0.51	1.46	0.00	13.89
humancap	1,290	43	3.05	0.52	1.77	3.97
spi	1,320	44	76.39	11.31	49.18	89.97
gdppc	1,320	44	35,776.08	23,690.32	4,441.42	96,477.22
ethnofrac	1,320	44	45.02	24.54	1.90	95.80
europe	1,320	44	0.43	0.49	0	1
northamerica	1,320	44	0.05	0.21	0	1
latinamerica	1,320	44	0.16	0.36	0	1
ssafrica	1,320	44	0.02	0.15	0	1
A-Driving	1,050	35	46.17	24.41	9.82	161.59
A-Transit	540	18	36.06	29.04	7.04	155.51
A-Walking	1,050	35	41.84	24.46	5.82	178.42
G-RetailRecreation	1,320	44	47.40	28.62	3.00	117.00
G-GroceryPharmacy	1,320	44	74.13	24.48	3.00	146.00
G-Parks	1,320	44	70.67	37.63	9.00	288.00
G-TransitStations	1,320	44	46.08	26.28	5.00	108.00
G-Workplace	1,320	44	57.12	24.42	8.00	104.00
G-Residential	1,320	44	119.42	11.20	98.00	153.00
Relative Output	425	20	89.30	9.55	62.66	114.77

Table B.3: Correlation Coefficients

Variables	(1)	(2)	(3)	(4)	(5)	(6)	(7)	(8)	(9)	(10)	(11)	(12)
(1) MIDIS	1.000											
(2) stringency	0.334	1.000										
(3) infected	0.141	0.021	1.000									
(4) deceased	0.142	0.052	0.806	1.000								
(5) humancap	-0.103	-0.350	0.107	0.079	1.000							
(6) spi	-0.136	-0.428	0.128	0.173	0.818	1.000						
(7) loggdppc	-0.163	-0.350	0.129	0.119	0.717	0.824	1.000					
(8) ethnofrac	-0.162	0.148	0.042	0.057	-0.362	-0.360	-0.284	1.000				
(9) europe	-0.071	-0.097	0.037	0.139	0.410	0.553	0.367	-0.370	1.000			
(10) northamerica	-0.236	-0.163	0.338	0.160	0.281	0.199	0.190	0.159	-0.190	1.000		
(11) latinamerica	-0.027	0.183	-0.107	-0.084	-0.211	-0.190	-0.294	0.170	-0.379	-0.095	1.000	
(12) ssafrica	0.125	0.103	-0.057	-0.051	-0.072	-0.140	-0.148	0.252	-0.133	-0.033	-0.066	1.000